A Study on Transient Grounding Performance of Ground Rods

윤동현 · 이형수 · 이관형
한국산업안전공단 산업안전보건연구원

1. Introduction

Although DC ground resistance is a good index of performance for a grounding system, it does not reflect the grounding performance during the transient states. Besides, impulse ground impedance, which is defined by a ratio of the peak value of transient ground potential rise to the peak value of impulse current, cannot be an absolute performance index due to its dependence on impulse current shape. In this paper, a grounding performance of needle-typed ground rod has been compared with simple ground rod using HIFREQ[1], which is an engineering electro-magnetic code based on MoM (Method of Moment).

2. Description of the Modeled Systems

2.1 Fundamental assumptions

Any aboveground structures that may be bonded to the rod were not considered in order to avoid diluting the significance of the comparison between the two types of rods. In the likely event that such aboveground structures may have a noticeable influence on the overall performance of the system that is subject to a lightning surge current. For the same reason, we will not consider the effects of other ground conductors (such as other ground rods, grounding grids, tower grounds, etc.) that may be connected to the ground rod. In other words, we assume that once lightning has hit a structure, the surge current starts flowing in all directions towards the buried ground conductors including the rod under investigation. We therefore assume that from the initial total surge current of Isurge(t) that struck the structure, a fraction βIsurge(t)(β where is a coefficient between 0 and 1) reaches the top of the rod as shown in the fig.1. We further assume that this coefficient is exactly the same for both types of rods analyzed in this report. That assumption is not necessarily true but is acceptable for the purpose of this analysis.

2.2 Configuration and Characteristics

Fig.2 shows the configuration and characteristics of the Simple and Needle rods. Both rods are made of a polyethylene rod covered with two concentric tubular metallic layers. The inner layer is made of aluminum and the outer layer is made of stainless steel. A preliminary investigation has determined that for the purpose of this study, a 14mm diameter tubular rod made of a 2mm thick aluminum wall is a good approximation over the entire range of the frequency spectrum covered by the lightning surge. That approximation avoids the cumbersome task of evaluating the equivalent uniform composite material to use at each frequency.

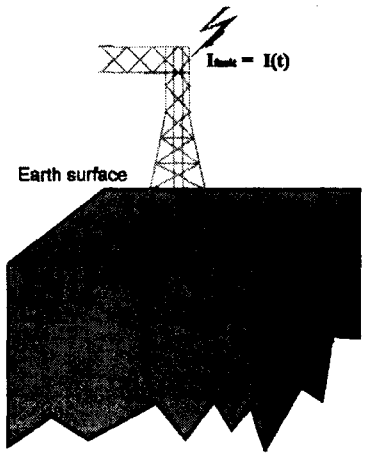

Fig. 1 Fundamental assumption

2.3 Soil Structure

The soil is assumed to be uniform with a 500 ohm-m resistivity and a relative permeability and permittivity of 1 for both parameters respectively. The top end of the rod lies on the surface of that soil.

2.4 Energization

The top end of the ground rod is energized with a double exponential lightning surge current as defined in the following FFTSES Forward Fourier Transform screen. The peak value of this current is about 30 kA. Wave shape of energization current is shown at Fig. 3.

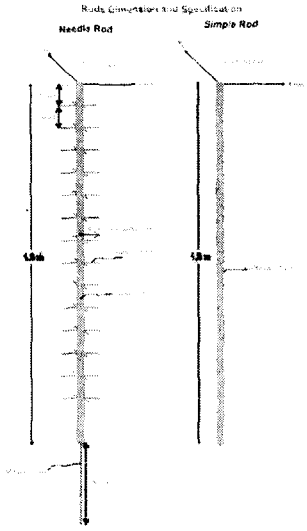

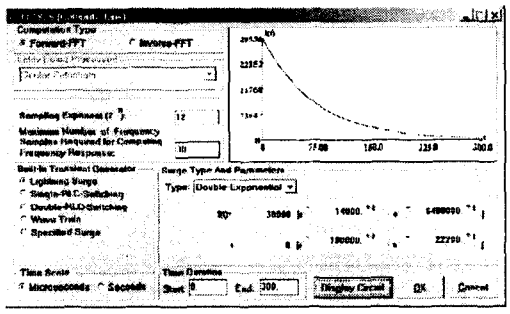

Fig.2 Configuration and Characteristics Fig.3 Wave shape of energizing current

2.5 Required Computation Results

In addition to the usual quantities such as conductor segment GPRs (Ground Potential Rise), a large number of observation points located in the vicinity of the rod surface for electric field calculation were calculated.

3. Description of the Computation Results

3.1 GPRs (Ground Potential Rise)

The time-domain GPR of the top end segment of the Simple and Needle rods are shown at Fig. 4 and 5, respectively. Although it is clear that the peak GPR value occurs almost at the same time as the lightning surge current peak (30,000A), there is nonetheless a small delay in the case of the needle rod. Furthermore, the magnitude of that peak is more than 8.3 MV for the simple rod and almost 7 MV for the needle rod.

3.2 Electric Fields in Earth

One of the main objectives of this project is to evaluate the location of maximum electric fields. Although the computation results provide all components (X, Y, Z) of the electric and magnetic fields, this brief report focuses on the resultant electric field, i.e..

(1) Simple Rod

Fig. 6 shows the resultant electric field around the Simple rod. It shows a 3D view of the time-domain field along a profile originating 1 mm away from the edge of the bottom end of the rod surface and terminating 35mm away. This Fig. clearly shows that the maximum electric field is about 260 MV 1mm away from the rod surface. The tip of the rod is the location of the highest electric field along the entire rod. Note that the maximum of the X, Y and Z components of the electric field do not occur all at the same point. The Z component however peaks at that same rod tip location. The other two components of the electric field peak are somewhere between the two ends (at about 1.55 m from the top).

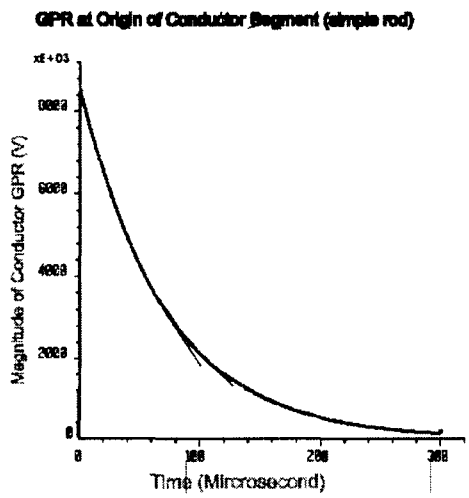

Fig. 4 GPR of the Simple Rod

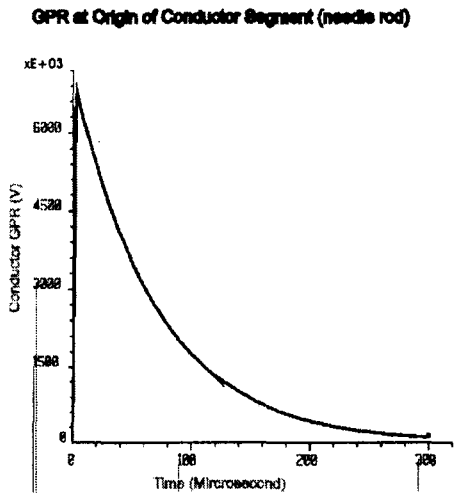

Fig. 5 GPR of the Needle Rod

(2) Needle Rod

Fig. 7 shows the resultant electric field around the Needle rod for profiles located on Surface 1. It shows a 3D view of the time-domain field along a profile originating 1 mm away from the edge of the rod and along (but 1 mm away) the last horizontal needle located close to the bottom end of the rod surface. The length of that profile is 70 mm. This figure clearly shows that the maximum electric field is about 315 MV at a location that is 32 mm away from the rod surface. That is the location of the highest electric field along the entire rod and needle surfaces except for the rod end (tip) needle. Note that the maximum of the X, Y and Z components of the electric field do not occur all at the same point.

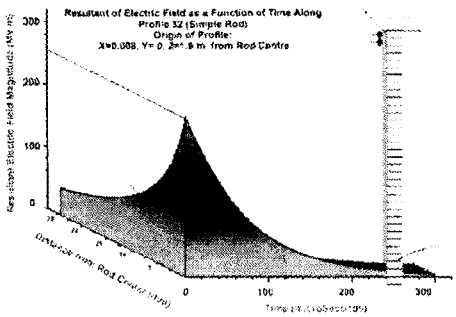

Fig. 6 Resultant Electric Field (Profile 32 Near a Simple Rod)

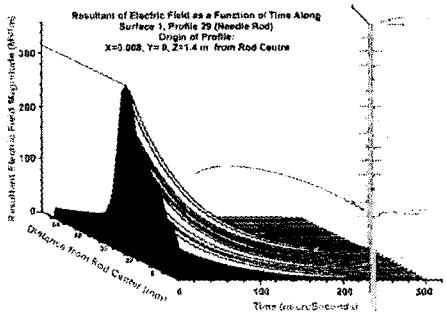

Fig. 7 Resultant Electric Field (Profile 29 Near a Needle Rod)

4. Conclusions and Recommendation

This study shows that the maximum electric field is definitely increased by a factor of 1.75, i.e., from 260 MV to 455 MV when we use a needle rod instead of a simple rod. This factor does not account for the extra length of material introduced by the needle. If the extra length is accounted for (i.e., 3.6m/1.6m = 2.25) an additional factor of 2.25 should be applied. In this case the field will be enhanced by factor of 4. Therefore, a Needle rod does amplify the electric fields sharply compared to a simple rod of equal overall length. The results of the computations show also that both rods behave as a resistor even at frequencies of about 6 MHz. Furthermore, the peak electric fields occur about 10% away from the ends of the horizontal needles and between 10 and 15% from the end of the vertical needle.

This study gathered extensive computation data that could not be processed in this limited study. Finally, as mentioned in the introduction, this study did not examine the influence of other buried and aboveground metallic conductors and structures that may affect the overall performance of the rods. This aspect must be studied for completeness.

References

[1] F. P. Dawalibi, F. Donoso, "Integrated Analysis Software for Grounding, EMF and EMI ", IEEE Computer Applications in Power, Vol. 6, No. 2, pp. 19-24.1993